J Musculoskelet Neuronal Interact 2010; 10(1):92-99

Original Article

Hylonome

Rapid vinculin exchange dynamics at focal adhesions in primary osteoblasts following shear flow stimulation

L. Tan[1], T. Meyer[2], B. Pfau[3], T. Hofmann[4], T.W. Tan[1], D. Jones[1]

[1]Institut für Experimentelle Orthopädie und Biomechanik, Universität Marburg; [2]Abteilung Kardiologie, Universität Marburg; [3]Helmholtz-Zentrum für Materialien und Energie, Berlin; [4]Institut für Pharmakologie und Toxikologie, Universität Marburg, Germany

Abstract

The adaptor protein vinculin plays a key position in the formation of focal adhesions and regulates cell attachment. To study the turnover of vinculin in bone-derived cells, we expressed green fluorescent protein-tagged vinculin in primary bovine osteoblasts and examined the appearance of focal adhesions in cells exposed to laminar shear flow. Already 20 sec after application of shear stress fluorescently labelled focal adhesions became visible as small flashing dots at the periphery of cells. The number of newly formed focal adhesions per individual cell increased continuously over approximately 300 sec and then remained relatively stable. The assembly of focal adhesions in shear stress-stimulated osteoblasts was accompanied by a transient rise in intracellular calcium levels. The mean assembly time of an individual focal adhesion plaque was 32.2±2.2 sec and the mean disassembly time was 60.5±6.0 sec. The recruitment of vinculin to nascent focal adhesions was in the same range as the recovery half-life of GFP-vinculin at stable focal adhesions (13.0±2.0 sec). These data show that accumulation of GFP-vinculin in newly formed focal adhesions and its exchange from pre-existing, mature plaques are both rapid processes that occur in mechanically stimulated osteoblasts within less than one minute.

Keywords: Vinculin, Focal Adhesions, Dynamics, Fluid Shear Stress, Osteoblasts

Introduction

Bone has a remarkable ability to adjust its mass and architecture in response to a changing mechanical environment. Living bone is permanently undergoing remodelling processes, which allow for a continuous fine tuning of the amount and spatial organization of calcified tissue in response to mechanical strain[1]. A variety of types and magnitudes of mechanical stimuli ranging from micro-gravity to hyperphysiological loads, including fluid shear, tensile and compressive strains, gravity and vibration, have been shown to influence bone cell metabolism[2,3]. In cooperation with embedded osteocytes, osteoblasts lining bone surfaces at sites of new bone formation are key players that change the matrix secretion and subsequent calcification upon mechanical stimulation[2-7].

The mechanisms by which mechanical stresses evoke biological responses in bone have been proposed to involve (a) direct deformations of cells via structural deformation of the bone matrix, (b) load-induced changes in the flow of interstitial fluid in canaliculi of osteons, or (c) streaming potentials[8]. Load-induced cell deformations and fluid shear stresses act directly on the apical cell surface. Bundles of actin filaments, which terminate at sites of rigid contacts between the cell and its surrounding microenvironment, may transmit mechanical forces acting on the apical membrane to the interior of the cell. The close contact of bone cells to matrix proteins requires at the intracellular site that transmembrane integrins are coupled to the actin cytoskeleton via components that are concentrated in focal adhesions such as talin, vinculin, paxillin and α-actinin[9-13]. The physical linkage of transmembrane receptors to the intracellular cytoskeleton may function as part of the mechanosensor that activates intracellular signalling pathways[14,15]. There is a growing body of evidence suggesting that cytoskeletal proteins have important roles in detecting and coordinating responsiveness to mechanical signals and that they communicate these signals to change bone metabolism[2-5,16]. Cytoskeletal rearrangements

The authors have no conflict of interest.

Corresponding author: Thomas Meyer, PhD, MD, Abteilung Kardiologie, Universität Marburg, Baldingerstraße 1, 35033 Marburg, Germany
E-mail: meyert@med.uni-marburg.de

Edited by: F. Rauch
Accepted 4 December 2009

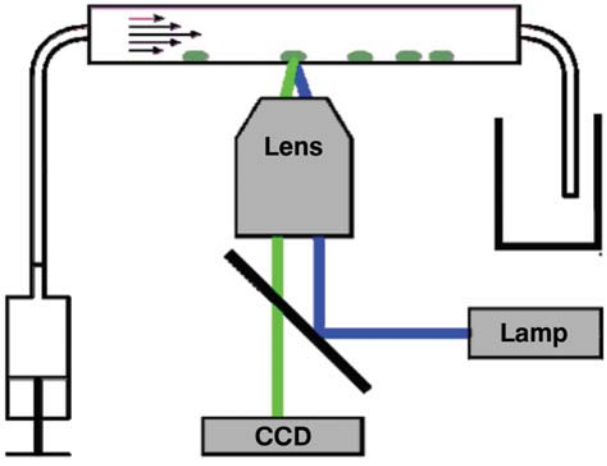

Figure 1. Experimental set-up for studying living osteoblasts under continuous laminar fluid shear stress. Osteoblasts were transfected with an expression plasmid coding for green fluorescent protein (GFP)-fused to vinculin and placed in a parallel-plate laminar flow chamber connected to a perfusion pump. Usually, cells were exposed to laminar shear flow of 1.5 N/cm^2 for 1 min and observed before and up to 30 min after stimulation using a fluorescence microscope equipped with appropriate fluorescence filters. Images from time series were captured and visualized using standard image software.

within focal adhesions provide a putative mechanism by which cell-matrix interactions could transduce and integrate the effects of strain into an intracellular response. The proposed role of focal adhesion components in mechanotransduction between the extracellular matrix and the cytoskeleton may go far beyond morphological changes and induce long-lasting alterations in gene expression profiles and matrix synthesis.

To better understand the dynamic features of focal adhesions in bone cells on a molecular level, we studied the formation, structural stability and dynamic exchange rate of vinculin at focal adhesion sites in primary osteoblasts exposed to shear stress. The data presented here demonstrate the fast formation and subsequent disassembly of focal adhesions in shear stress-stimulated osteoblasts. Moreover, we revealed the rapid accumulation and turnover of vinculin at focal adhesions in mechanically stressed primary osteoblasts. This unexpected high exchange rate of vinculin reflects the fast emergence of these transient, highly versatile adhesive structures at the cell-matrix interface.

Materials and methods

Cell culture and transfection

Bovine primary osteoblasts were prepared using an outgrowth method[17]. Briefly, periosteum pieces from bovine ulnae and radii were obtained at the local slaughterhouse and all soft tissue was removed. The periost pieces were placed under sterile conditions in Petri plates for 3-4 weeks. Cells were cultured in BGJb medium with Fitton-Jackson modification supplemented with 10% foetal calf serum in a humidified atmosphere of 5% CO_2/95% air at 37°C. The outgrowth of cells led to a homogeneous culture of bovine primary osteoblasts. Osteosarcoma cells of the MG63 cell line were obtained from the American Tissue Culture Collection and grown in RPMI 1640 medium (Sigma)[18]. Cells were transfected with a pEGFP-C1 expression vector coding for a fusion protein of green fluorescent protein (GFP) and vinculin under the transcriptional control of the human cytomegalovirus immediate early promoter (Tova Volberg, Weizmann Institute, Israel). Transfection was carried out with the Nanofectin kit (PAA) according to the manufacturer's recommendations.

Shear flow stimulation

For direct localization of GFP-tagged vinculin, transiently transfected bovine primary osteoblasts cells were placed in a parallel-plate fluid chamber connected with a perfusion pump (Figure 1)[19]. Usually, cells were incubated with 10 mM HEPES in Ham's medium (Biochrom) and pre-exposed to shear stress of 0.04 N/m^2 before they were stimulated for 1 min with laminar shear flow of 1.5 N/m^2. Cells were observed for 30 min after stimulation using phase contrast microscopy and direct fluorescence imaging in an inverse Nikon Diaphot fluorescence microscope equipped with appropriate fluorescence filters. Fields of view for image acquisition were chosen in central regions of the plate where a fully developed laminar flow existed and GFP-vinculin-expressing cells were present. Images were obtained with a Xillix CCD camera and further processed with the software program Image-Pro-Plus (Media Cybernetics).

Immunocytochemical staining

The intracellular distribution of vinculin in mechanically stimulated and unstimulated osteoblasts was determined by means of immunocytochemistry. Cells were either exposed to laminar fluid shear stress using 1.5 N/m^2 or left untreated. Cells were fixed with acetone/methanol (1:1) at -20°C and permeabilized with 0.2% Triton X-100 in phosphate-buffered saline (PBS). After three washes in 0.1% Triton X-100/PBS, monoclonal anti-vinculin antibody (Sigma) was added and incubated overnight at 4°C. The samples were washed three times in 0.1% Triton X-100/PBS and then incubated with fluorescein isothiocyanate (FITC)-labelled secondary antibody for 60 min at room temperature. Finally, samples were rinsed three times with water and mounted in fluorescence mounting medium. Fluorescence microscopy was performed using a Nikon Diaphot fluorescence microscope and filters selectively detecting FITC/GFP. The mean life time of a single focal adhesion in shear stress-stimulated cells was determined by means of the half-width of the half amplitude method separately for the assembly and disassembly of focal adhesions.

Traction measurement and force calculation

Bovine primary osteoblasts were grown on collagen-coated flexible polyacrylamide sheets with embedded fluorescent marker beads at a density of 3000 cells/cm^2 [20,21]. The substrate

contained 2% of a 1:3 mixture of 0.2 μm and 0.5 μm fluorescent latex microbeads (FluoSpheres, Molecular Probes). A volume of 12 μl was used for substrates covered with round coverslips (14 mm diameter). Coverslips were coated with type-I collagen as described by Wang and Pelham[20]. The mechanical properties of the gel allowed the cell to deform the substratum. The gel relaxed and the marker beads resumed their initial position when the cell was removed. Bead displacements were extracted automatically from the fluorescence micrograph time series. Deformations of the substrate were calculated as a matrix of vectors by comparing the fluorescent-light patterns caused by the embedded beads in the presence and absence of the cell[21,22]. For force calculations the LIBTRC software based on a Linux platform obtained from Dr. Micah Dembo (Boston University, MA, USA) was used[23,24].

Measurement of calcium concentrations

Intracellular calcium concentrations were measured in osteoblasts grown on glass coverslips. Briefly, cells were incubated for 90 min with either 3 μM Fluo-3/AM or 3 μM Calcium Green 1/AM (both obtained from Molecular Probes) in Ham's medium supplemented with 10 mM HEPES[25]. The dye-loaded cells were excited at 488 nm and the fluorescence was measured through a long-pass filter (510 nm) on an inverted microscope. Intracellular Ca^{2+} concentrations were measured before and after shear stress application or treatment with 5 μM thapsigargin (Molecular Probes). The increase in intracellular Ca^{2+} concentrations in response to cell stimulation was detected in groups of 10-20 dye-loaded cells, which were randomly selected in each experiment.

Fluorescence recovery after photo-bleaching (FRAP)

FRAP studies were conducted on live osteoblasts expressing GFP-tagged vinculin. A LSM510 inverted confocal laser scanning microscope (Carl Zeiss Jena) with a ×100/1.3 objective was used with an argon laser (λ=488 nm) as excitation source. Regions of interest (ROIs) containing one or several focal adhesions were bleached for 10-30 sec by high-intensity laser application. The time course of the fluorescence recovery of GFP-vinculin was tracked by an attenuated monitoring beam each for 130 sec. Fluorescence intensity differences between unbleached ROI and adjoining bleached ROI were calculated and used for an exponential curve fitting to estimate recovery times of GFP-tagged vinculin. For determination of the recovery half-life, the normalized recovery curve was fitted to a single exponential recovery model using the equation: $F_t = F_f-(F_f-F_i)e^{-k/t}$, where F_i is the fluorescence intensity at time t, F_f is the final fluorescence at the plateau phase, F_i is the initial fluorescence extrapolated to t=0 after photobleaching, and k=ln $2/t_{1/2}$.

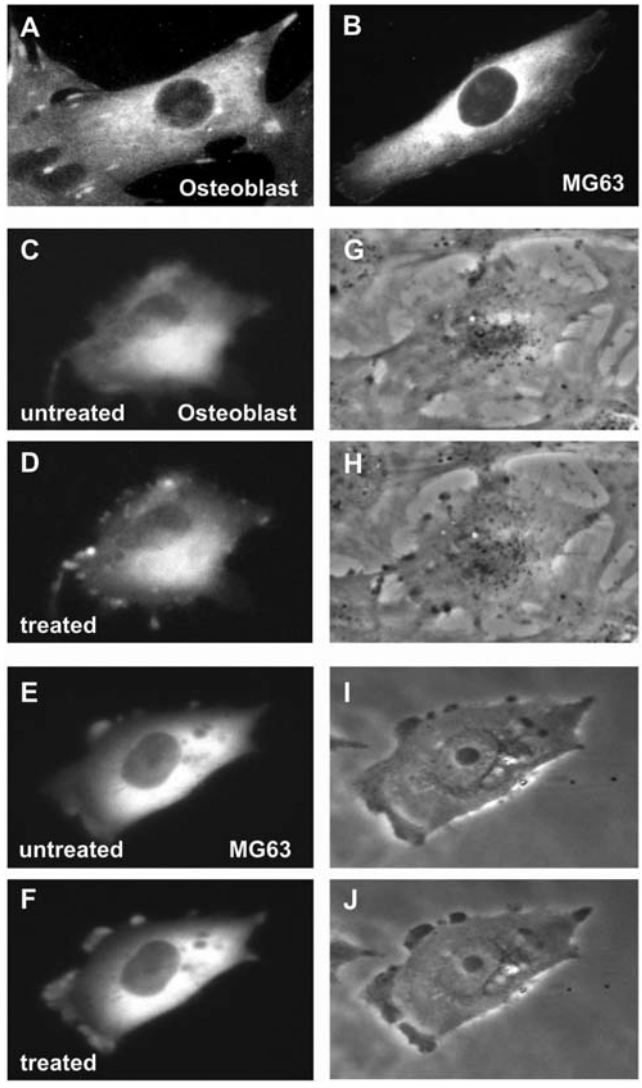

Figure 2. Intracellular localization of native and recombinant GFP-tagged vinculin in primary bovine osteoblasts and osteosarcoma-derived MG63 cells, before (C,E,G,I) and after exposure to shear flow (A,B,D,F,H,J). Cells expressing a GFP-tagged fusion protein of vinculin were stimulated with laminar shear flow of 1.5 N/m^2 and subsequently either fixed for immuncytochemical labelling (A,B) or proceeded for direct microscopical observation (C-J). (A,B) Immunocytochemical staining of endogenous vinculin in stimulated cells using monoclonal anti-vinculin antibody and fluorescein isothiocyanate (FITC)-labeled secondary antibody. (C-F) Distribution of GFP-tagged vinculin in transfected osteoblasts and MG63 cells, before (C,E) and after stimulation (D,F). (G-J) Phase contrast microscopical imagines of the corresponding cells shown in C-F. Note that the cell-type specific staining pattern of vinculin did not differ between the native protein and its recombinant GFP counterpart and that vinculin redistributed to focal adhesions upon mechanical stimulation.

Results

To visualize the subcellular distribution of vinculin in shear flow-stimulated bone-derived cells, we exposed primary osteoblasts and osteosarcoma-derived MG63 cells to laminar shear flow of 1.5 N/m^2. Before and after 30 min stimulation we followed vinculin redistribution by means of two independent fluorescence techniques, namely immunocytochemical labelling of endogenous vinculin and transfection of an expression plasmid coding for vinculin fused to green fluores-

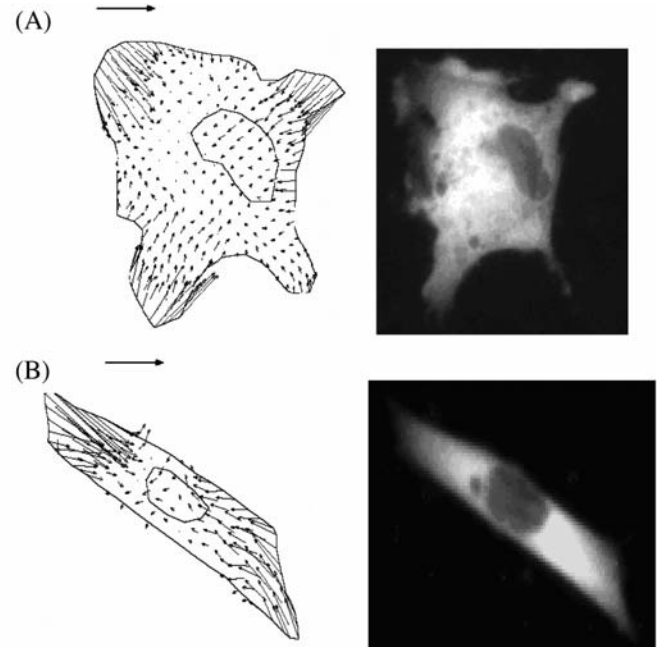

Figure 3. Traction force measurements in primary bovine osteoblasts (**A**) and osteosarcoma-derived MG63 cells (**B**) grown on collagen-coated flexible polyacrylamide sheets with embedded fluorescent marker beads. For force calculation, substrate deformations of cells were quantified by marker bead displacement. Images were taken from time-lapse acquisitions and the spatial distribution of traction forces within each cell was determined as a matrix of vectors. The arrow lengths above each cell indicate a traction force value of 0.1 N/cm^2 (**A**) and 0.06 N/cm^2 (**B**), respectively.

cent protein (GFP). Indirect immunofluorescence staining with a monoclonal anti-vinculin antibody revealed a homogeneous distribution of endogenous vinculin in the cytoplasm of both cell types, while in the nucleus, positive immunolabelling was missing (Figure 2A,B). The intensity of cytoplasmic vinculin labelling was similar in both cell types. Besides this pancellular cytosolic fluorescent signal, we detected vinculin in discrete spots corresponding to focal adhesion plaques at the cell-matrix interface following shear flow exposure. The association of vinculin with focal adhesions was most prominent in spreading bovine primary osteoblasts and was less intense in MG63 cells, which usually displayed a more spheroidal, less flattened cell shape. In MG63 cells the number of focal adhesions per single cell and the spatial extent of each individual focal adhesion plaque were frequently reduced as compared to those in primary osteoblasts (Figure 2A,B).

The expression of GFP-vinculin in bone-derived cells closely resembled the partitioning of the native vinculin in two independent intracellular pools (Figure 2C-F). After mechanical stimulation a patchy staining pattern associated with focal adhesions and a homogeneous distribution throughout the cytosol leaving out the nucleus were observed (Figure 2D,F). Again, we found that MG63 osteosarcoma cells displayed significantly fewer and smaller focal adhesions at the substratum, both before and after stimulation. Interestingly, upon shear flow stimulation GFP-tagged vinculin concentrated in streak-like structures at the periphery of the cells (Figure 2D,F). The accumulation of vinculin in these focal adhesions was usually more prominent in primary osteoblasts than in MG63 cells. Phase contrast microscopy confirmed that primary osteoblasts exhibited a higher number of focal adhesions, which appeared as black elongated structures oriented in the direction of stress fibres or as round dots at the edge of the cell (Figure 2G-J).

We then calculated traction forces of unstimulated bone-derived cells cultivated on collagen-coated flexible polyacrylamide sheets containing fluorescent marker beads by analyzing substrate deformation. Traction forces applied by the cell were quantified by the displacement of the fluorescent marker beads embedded in the gel[20,26]. The spatial distribution of traction forces was analysed by comparing the fluorescence light patterns obtained from embedded beads in the presence or absence of cells. The data were presented as a matrix of vectors within the cell[24]. The most prominent deformations were found at the edge of the cell (Figure 3). The mean traction forces in stationary phase transmitted by primary osteoblasts were generally higher as compared to MG63 cells (2.5 μN/cell versus 0.5 μN/cell; n=23 each; p=0.015).

Additionally, we examined the role of intracellular calcium transients in shear stress-stimulated osteoblasts. Calcium Green-1 and Fluo3-AM-loaded cells were exposed to two magnitudes of fluid shear stress (1.5 and 3.0 N/cm^2, respectively) and the changes in the intracellular Ca^{2+} concentrations were monitored microscopically using the calcium indicator dye. At both stress magnitudes applied, we detected a significant elevation in intracellular Ca^{2+} levels. However, the rise in the cytoplasmic Ca^{2+} concentrations tended to be low and transient with only an 1.1-fold elevation as compared to resting cells. The shear stress-induced Ca^{2+} peak lasted up to 150 sec after shear stress stimulation. In control experiments, we treated cells with 5 μM of the tumour promoter thapsigargin, which specifically inhibits endoplasmic reticulum Ca^{2+}-ATPases and, thereby, depletes intracellular calcium stores[27]. Within 15 sec of stimulation with thapsigargin, a detectable peak in the cytosolic and, even more, the nuclear Ca^{2+} concentration was observed. We observed a 1.3-fold rise in the cytoplasmic fluorescence signals in response to stimulation with thapsigarin.

We next investigated the time course of shear stress-induced focal adhesion assembly in primary osteoblasts grown in parallel-plate flow chambers. In subconfluent layers of cells expressing GFP-vinculin, time-lapse image sequences were acquired at 10 sec intervals for 10 min before and after the onset of steady unidirectional shear stress (1.5 N/m^2), which was applied by a perfusion pump for 1 min. Observations of the GFP fluorescence signals together with phase contrast microscopy allowed the monitoring of the dynamic assembly of focal adhesions in stressed cells (Figure 4). Phase contrast microscopical images demonstrated that the gross cell morphology including shear stress-induced edge ruffling and lamellipodial protrusions were indistinguishable from trans-

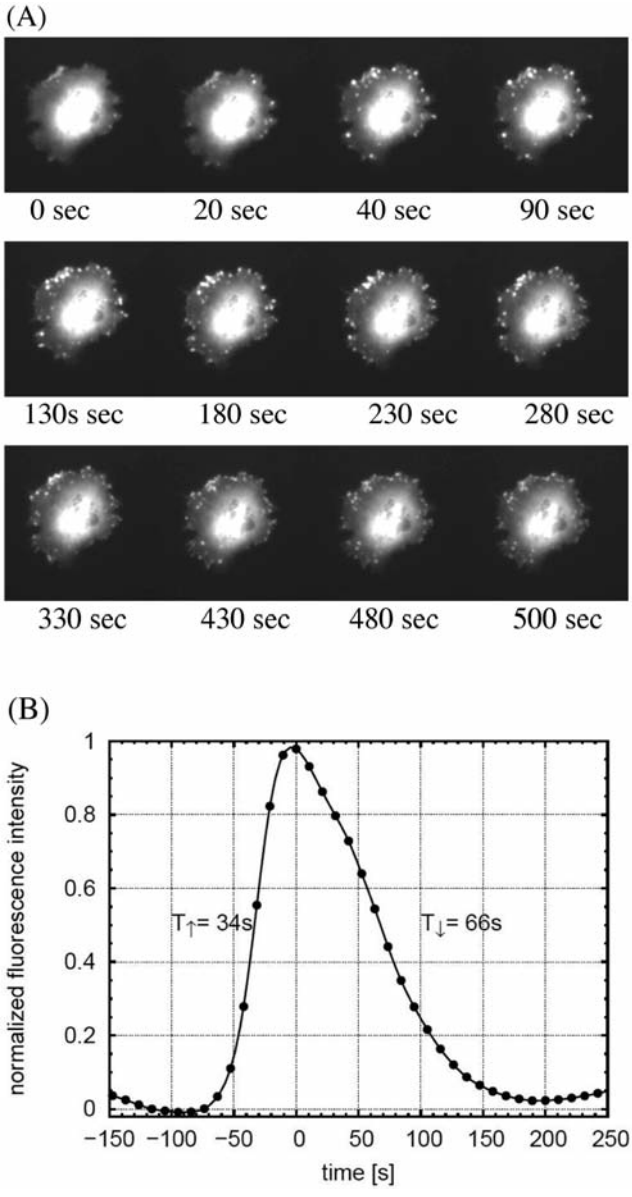

Figure 4. Effects of shear stress on the distribution of vinculin in primary bovine osteoblasts. (**A**) Time series of focal adhesion formation in a GFP-vinculin-expressing osteoblast exposed to laminar fluid shear stress. Osteoblasts were transfected with an expression plasmid coding for GFP-tagged vinculin and placed in a parallel-plate fluid chamber to allow the application of constant laminar shear flow (1.5 N/m^2 for 1 min). Fluorescence micrographs depict the intracellular distribution of a representative single cell before and at the indicated times given in seconds after shear stress application. (**B**) Time course of the integrated fluorescence intensity in a typical individual focal adhesion site. From the average time profile of a single focal adhesion flash, a formation time of 32.2±2.2 sec and a mean disassembly time of 60.5±6.0 sec were calculated.

fected and adjacent non-transfected cells. Within 10 sec of the onset of shear stress application, lamellipodial extensions appeared at the rim of the cells and, after a delay of approximately 20 sec beginning with the start of the stimulation (time zero), fluorescently labelled focal adhesion plaques were visible, which appeared as flashing dots at the periphery of cells (Figure 4A). Green fluorescent protein-tagged vinculin accumulated at focal adhesion plaques in distinct punctate spots and not in streak-like elongations. The number of newly formed vinculin-positive focal adhesions sites per individual cell increased continuously over approximately 300 sec. The number of focal adhesion complexes per individual cell then reached a plateau phase and, after 400-500 sec, decreased slowly until the end of the observation period. Despite the changing number of focal adhesions, the spatial extent of each individual focal adhesion plaque remained remarkably uniform at different times after stimulation. We found that the de-novo assembly and growth of focal adhesions in shear stress-exposed osteoblasts were rather fast processes. Using time-lapse video recording, the mean assembly time of an individual focal adhesion plaque was measured to be 32.2±2.2 sec and the mean disassembly time was 60.5±6.0 sec (Figure 4B).

Finally, we assessed the exchange rate of GFP-vinculin at mature focal adhesion plaques as a measure of focal adhesion turnover using FRAP analysis. Single focal adhesions localized at the periphery of the cell were bleached by high-intensity laser irradiation and the recovery of GFP fluorescence was monitored over a period of 130 sec. The measured recovery half-life of GFP-vinculin ranged from 10.4 sec to 16.4 sec with a mean and standard deviation of 13.0±2.0 sec (Figure 5). This compared well with the estimated formation time of focal adhesions in shear stress-stimulated osteoblasts, as described above (see Figure 4B). Thus, the accumulation of GFP-vinculin in newly formed focal adhesions and its recruitment to pre-existing mature plaques are both rapid processes that occur in less than 1 minute.

Discussion

In the study presented, we investigated the dynamic assembly of focal adhesion sites in primary bovine osteoblasts exposed to mechanical strain. Fluorescent imaging of GFP-tagged vinculin was used to record the formation of adhesion sites in cultivated osteoblasts stimulated with fluid shear stress and to estimate the vinculin exchange rate in pre-existing adhesion sites. The major finding of our study is the rapid recruitment of GFP-vinculin to both newly formed as well as stationary focal adhesion sites in primary osteoblasts. We found that the accumulation of GFP-vinculin in de-novo formed and stable focal adhesions occurred within the same range as determined from time-lapse recordings and FRAP analyses, respectively. Using different fluorescence techniques, we calculated the half-lives of both processes to be less than 60 sec, indicating that GFP-vinculin is incorporated with high exchange rates in both nascent and mature focal adhesion sites. From our data it appeared as if the homogeneously dis-

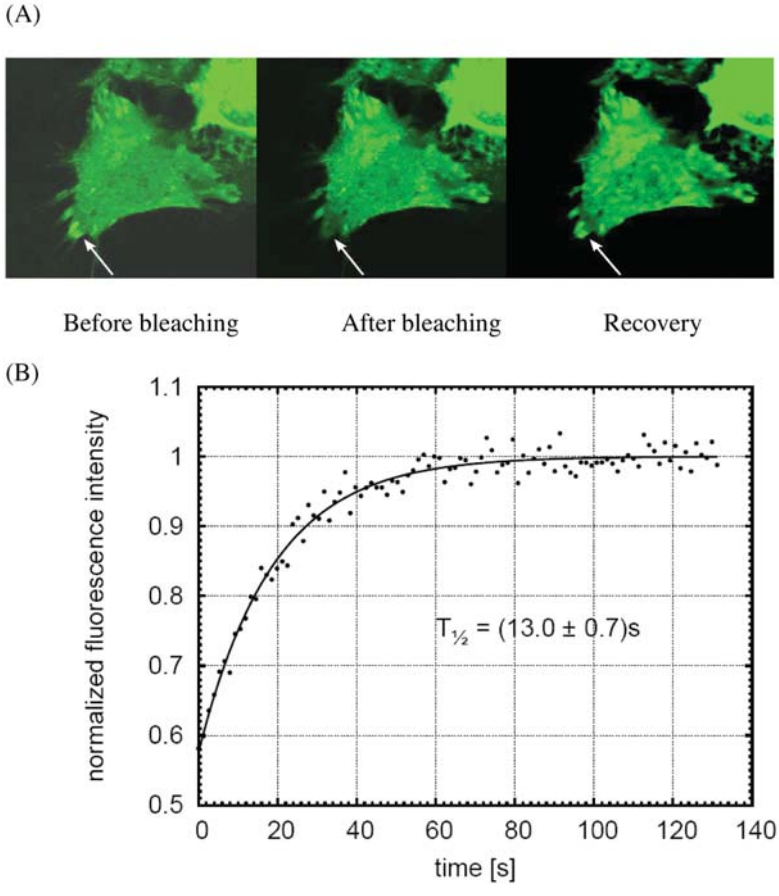

Figure 5. Rapid exchange of vinculin from focal adhesions in osteoblasts as revealed by FRAP analysis. Fluorescence recovery after photobleaching was performed in cultured osteoblasts expressing GFP-tagged vinculin. Regions of interest (ROIs) containing one or several focal adhesions were bleached by high-intensity laser irradiation and the recovery of GFP-vinculin fluorescence was monitored for 130 sec. (**A**) The micrographs show the ROI in a target cell before (left), immediately after (middle) and 60 sec after bleaching (right). (**B**) Typical fluorescence recovery curve of a bleached ROI with an exponential fitting of the data.

tributed vinculin in the cytosol functions as an exchangeable pool for the assembly of immature and the maintenance of mature focal adhesion sites. The measured rapid accumulation and exchange rates of focal adhesion-associated vinculin in osteoblasts point to a structural role of vinculin in cellular processes engaged in the attachment to extracellular matrix components[9,11,16,28].

There is a growing body of evidence demonstrating the role of vinculin and other focal adhesion-associated proteins in coordinated cell adhesion and migration, but most of these studies were performed in cells other than bone-derived cells[9,11,28]. Vinculin has been assigned a key position regulating focal adhesion formation and turnover in a variety of cells[11]. Numerous studies have shown that focal adhesion sites couple the actin network to extracellular matrix molecules, thereby generating tractional forces for cell locomotion and morphological changes that accompany cell movement on the substratum[4,14,29-31]. Our data on traction forces in two different bone-derived cell types are consistent with previous observations showing that the orientation of focal adhesions is collinear with the direction of force application on the extracellular matrix[21,31]. The number of focal adhesions per cell and the magnitude of traction forces appeared to correlate with each other: primary osteoblasts frequently showed more focal adhesion sites per individual cell and generally displayed higher traction forces as compared to osteosarcoma-derived MG63 cells.

Based on FRAP analyses and mathematical simulation, Wolfenson et al. have identified the juxtamembrane region surrounding focal adhesions as an intermediary layer with a gradient of focal adhesion proteins that enables efficient regulation and reorganization of focal adhesions[32]. Recently, Möhl and colleagues have demonstrated a correlation between vinculin exchange dynamics and adhesion strength during maturation of focal contacts in keratinocytes[15]. For nascent focal adhesions in moving keratinocytes, the authors determined a higher exchangeable vinculin fraction and lower recovery half-life as compared to stable focal adhesions of stationary cells. Additionally, they reported that, in these cells, the fraction of

stably incorporated vinculin increased with cell forces and decreased with vinculin phosphorylation. Because in our study we did not attempt to distinguish between different maturation states of focal adhesion sites, we are unable to confirm these findings in osteoblasts.

Additionally, we addressed the role of calcium in osteoblasts exposed to fluid shear stress. We found that osteoblasts sensitive to shear stress reacted with a low and transient increase in intracellular calcium levels. These weak flow-induced calcium peaks occurred simultaneously with the appearance of newly formed focal adhesions at the periphery of the cells. In thapsigargin-treated osteoblasts we detected a higher rise in intracellular Ca^{2+} concentrations, which was most prominent in the nucleus, suggesting that Ca^{2+} can rapidly diffuse between the cytoplasm and nucleoplasm. However, the functional role of calcium in the de-novo assembly of focal adhesions remains to be elucidated. Particularly, it will be interesting to know if changes in the intracellular calcium concentration are required for the orchestrated assembly and disassembly of vinculin-containing focal adhesions[33].

In summary, our data demonstrate the rapid recruitment of vinculin to nascent and mature focal adhesions in cultured osteoblasts upon exposure to shear stress. Although focal adhesions are relatively stable structures and the amount of incorporated vinculin is remarkably constant over time, vinculin exchanges at high rates from an unbound cytosolic pool to an ordered clustering at focal adhesions, and vice versa. The accumulation of vinculin in focal adhesions upon stimulation with shear stress is accompanied by a transient and weak release of intracellular calcium.

References

1. Gupta HS, Seto J, Wagermaier W, Zaslansky P, Boesecke P, Fratzl P. Cooperative deformation of mineral and collagen in bone at the nanoscale. Proc Natl Acad Sci USA 2006;103:17741-6.
2. Guignandon A, Akhouayri O, Usson Y, Rattner A, Laroche N, Lafage-Proust MH, Alexandre C, Vico L. Focal contact clustering in osteoblastic cells under mechanical stresses: microgravity and cyclic deformation. Cell Commun Adhes 2003;10:69-83.
3. Sugawara Y, Ando R, Kamioka H, Ishihara Y, Murshid SA, Hashimoto K, Kataoka N, Tsujioka K, Kajiya F, Yamashiro T, Takano-Yamamoto T. The alteration of a mechanical property of bone cells during the process of changing from osteoblasts to osteocytes. Bone 2008;43:19-24.
4. Meazzini MC, Toma CD, Schaffer JL, Gray ML, Gerstenfeld LC. Osteoblast cytoskeletal modulation in response to mechanical strain *in vitro*. J Orthop Res 1998;16:170-80.
5. Okumura A, Goto M, Goto T, Yoshinari M, Masuko S, Katsuki T, Tanaka T. Substrate affects the initial attachment and subsequent behavior of human osteoblastic cells (Saos-2). Biomaterials 2001;22:2263-71.
6. Diener A, Nebe B, Lüthen F, Becker P, Beck U, Neumann HG, Rychly J. Control of focal adhesion dynamics by material surface characteristics. Biomaterials 2005;26:383-92.
7. Woodruff MA, Jones P, Farrar D, Grant DM, Scotchford CA. Human osteoblast cell spreading and vinculin expression upon biomaterial surfaces. J Mol Histol 2007; 38:491-9.
8. Aarden EM, Nijweide PJ, van der Plas A, Alblas MJ, Mackie EJ, Horton MA, Helfrich MH. Adhesive properties of isolated chick osteocytes *in vitro*. Bone 1996; 18:305-13.
9. Chen H, Cohen DM, Choudhury DM, Kioka N, Craig SW. Spatial distribution and functional significance of activated vinculin in living cells. J Cell Biol 2005;169:459-70.
10. Cohen DM, Kutscher B, Chen H, Murphy DB, Craig SW. A conformational switch in vinculin drives formation and dynamics of a talin-vinculin complex at focal adhesions. J Biol Chem 2006;281:16006-15.
11. Humphries JD, Wang P, Streuli C, Geiger B, Humphries MJ, Ballestrem C. Vinculin controls focal adhesion formation by direct interactions with talin and actin. J Cell Biol 2007;179:1043-57.
12. Hytönen VP, Vogel V. How force might activate talin's vinculin binding sites: SMD reveals a structural mechanism. PLoS Comput Biol 2008;4:e24.
13. Digman MA, Wiseman PW, Choi C, Horwitz AR, Gratton E. Stoichiometry of molecular complexes at adhesions in living cells. Proc Natl Acad Sci USA 2009;106:2170-5.
14. Riveline D, Zamir E, Balaban NQ, Schwarz US, Ishizaki T, Narumiya S, Kam Z, Geiger B, Bershadsky AD. Focal contacts as mechanosensors: externally applied local mechanical force induces growth of focal contacts by an mDia1-dependent and ROCK-independent mechanism. J Cell Biol 2001;153:1175-86.
15. Möhl CC, Kirchgeßner N, Schäfer C, Küpper K, Born S, Diez G, Goldmann WH, Merkel R, Hoffmann B. Becoming stable and strong: the interplay between vinculin exchange dynamics and adhesion strength during adhesion site maturation. Cell Motil Cytoskeleton 2009;66:350-64.
16. Shemesh T, Geiger B, Bershadsky AD, Kozlov MM. Focal adhesions as mechanosensors: a physical mechanism. Proc Natl Acad Sci USA 2005;102:12383-8.
17. Schirrmacher K, Schmitz I, Winterhager E, Traub O, Brümmer F, Jones D, Bingmann D. Characterization of gap junctions between osteoblast-like cells in culture. Calcif Tissue Int 1992;51:285-90.
18. Billiau A, Edy VG, Heremans H, van Damme J, Desmyter J, Georgiades JA, de Somer P. Human interferon: mass production in a newly established cell line, MG-63. Antimicrobial Agents Chemother 1977;12:11-5.
19. Usami S, Chen HH, Zhao Y, Chien S, Skalak R. Design and construction of a linear shear stress flow chamber. Ann Biomed Eng 1993;21:77-83.
20. Wang YL, Pelham RJ Jr. Preparation of a flexible, porous polyacrylamide substrate for mechanical studies of cultured cells. Methods Enzymol 1998;298:489-96.
21. Balaban NQ, Schwarz US, Riveline D, Goichberg P, Tzur G,

Sabanay I, Mahalu D, Safran S, Bershadsky A, Addadi L, Geiger B. Force and focal adhesion assembly: a close relationship studied using elastic micropatterned substrates. Nature Cell Biol 2001;3:466-72.
22. Schwarz US, Balaban NQ, Riveline D, Bershadsky A, Geiger B, Safran SA. Calculation of forces at focal adhesions from elastic substrate data: the effect of localized force and the need for regularization. Biophys J 2002;83:1380-94.
23. Dembo M, Wang YL. Stresses at the cell-to-substrate interface during locomotion of fibroblasts. Biophys J 1999;76:2307-16.
24. Marganski WA, Dembo M, Wang YL. Measurements of cell-generated deformations on flexible substrata using correlation-based optical flow. Methods Enzymol 2003;361:197-211.
25. Lloyd QP, Kuhn MA, Gay CV. Characterization of calcium translocation across the plasma membrane of primary osteoblasts using a lipophilic calcium-sensitive fluorescent dye, calcium green C_{18}. J Biol Chem 1995; 270:22445-51.
26. Munevar S, Wang Y, Dembo, M. Traction force microscopy of migrating normal and H-ras transformed 3T3 fibroblasts. Biophys J 2001;80:1744–57.
27. Treiman M, Caspersen C, Christensen SB. A tool coming of age: thapsigargin as an inhibitor of sarco-endoplasmic reticulum Ca^{2+}-ATPases. Trends Pharmacol Sci 1998; 19:131-5.
28. Saunders RM, Holt MR, Jennings L, Sutton DH, Barsukov IL, Bobkov A, Liddington RC, Adamson EA, Dunn GA, Critchley DR. Role of vinculin in regulating focal adhesion turnover. Eur J Cell Biol 2006;85:487-500.
29. Pelham RJ Jr, Wang Y. Cell locomotion and focal adhesions are regulated by substrate flexibility. Proc Natl Acad Sci USA 1997;94:13661-5.
30. Zamir E, Geiger B. Molecular complexity and dynamics of cell-matrix adhesions. J Cell Sci 2001;114:3583-90.
31. Curtze S, Dembo M, Miron M, Jones DB. Dynamic changes in traction forces with DC electric field in osteoblasts-like cells. J Cell Sci 2004;117:2721-9.
32. Wolfenson H, Lubelski A, Regev T, Klafter J, Henis YI, Geiger B. A role for the juxtamembrane cytoplasm in the molecular dynamics of focal adhesions. PLoS One 2009;4:e4304.
33. Kamioka H, Sugawara Y, Murshid SA, Ishihara Y, Honjo T, Takano-Yamamoto T. Fluid shear stress induces less calcium response in a single primary osteocyte than in a single osteoblast: implication of different focal adhesion formation. J Bone Miner Res 2006;21:1012-21.